

# Chapter 3

## Mechanical Characterization and Process Optimization of PolyJet 3D Printing Using Digital ABS with Different Part Geometries



B. N. Sontakke and B. B. Ahuja

**Abstract** Last few decades have seen a rapid growth in additive manufacturing (AM) owing to its adaptability to new manufacturing requirement and trends. In PolyJet technology, a popular method in AM, parts are manufactured by depositing layer upon layer and, simultaneously, each layer is cured using ultraviolet energy. This process exhibits the structured approach of layered manufacturing process which produces state-of-the-art products with superior quality. The process has shown promising technological development in the field of design and manufacturing. This work aims at improving the performance characteristic and process optimization through the application of design of experiment approach. The response parameters viz. the storage modulus, loss modulus, loss factor, glass transition temperature, and surface roughness have been individually assessed. The statistical technique has been used to study the effect of process parameters and their significance. Gray relation grade analysis has been used for process optimization.

**Keywords** Additive manufacturing · PolyJet · Design of experiment · Dynamic mechanical analyzer · Surface roughness

### 3.1 Introduction

The manufacturing sector is passing through a phase where technological innovations demand shorter product development and manufacturing time along with faster product availability to market. Subtractive manufacturing has limitations in terms of product size, complexity, material loss, and high cost. These limitations have given a new direction to additive manufacturing, which offers rapid R&D, high complexity, and versatility. AM process basically builds the product by joining layer upon layer of required material and suits regular as well as complex products equally. The physical appearance and mechanical properties of parts manufactured by an

---

B. N. Sontakke · B. B. Ahuja (✉)

Department of Production Engineering and Industrial Management, College of Engineering Pune, Pune 411005, India

e-mail: [director@coep.ac.in](mailto:director@coep.ac.in)

© Springer Nature Singapore Pte Ltd. 2020

M. S. Shunmugam and M. Kanthababu (eds.), *Advances in Additive Manufacturing and Joining*, Lecture Notes on Multidisciplinary Industrial Engineering,

[https://doi.org/10.1007/978-981-32-9433-2\\_3](https://doi.org/10.1007/978-981-32-9433-2_3)

AM process are mainly characterized by machine parameters and material used. The mechanical properties of parts need to be investigated thoroughly in order to justify the inadvertent use of AM machines.

The past decade has shown a growing interest of researchers in AM processes which helps in significant improvement in mechanical properties, reliability, and repeatability of AM processes [1]. Make to order a customized product which will be the future market scenario can be easily fulfilled by AM processes [2]. Due to the short span between design and manufacturing, this process is also defined as rapid manufacturing [3]. AM machines are available in wide varieties are capable to process different materials and geometries. AM process is making progress to tackle current issues but needs substantial product improvements in terms of quality and cost including the production time [4]. Performance parameters of the AM process need to be competent which require processing simplification and standardization, which in turn attracts manufacturers and customers [5]. Today, industries such as aerospace, automotive, defense, and medical as well as consumer electronics which are producing quite regulated, demand-customized, geometrically, and mechanically stable components. Dimensional and surface topologies are two important aspects that have the substantial impact on the application of AM machines for production. These aspects are largely dependent on the part location of the geometry, on the build tray as well as the quality of the digital material. In-depth experimental investigations need to be carried out considering these aspects of the AM process which enable simplification and standardization [6–8]. Fused deposition modeling (FDM), selective laser sintering (SLS), stereolithography (SLA), and PolyJet technology are the most promising and innovative technological developments which will cater the growing demand for customized make to order situation prevalent in today's engineering market [9].

In this work, additive manufacturing (AM), using PolyJet process shown in Fig. 3.1, has been studied and an attempt has been made to investigate the influence of process parameters on product quality. The Taguchi method which is popular offline quality improvement method and needs a less number of experiments for a detailed analysis of the process has been used in this work. A single objective optimization of individual process parameters using the Taguchi method is proposed herewith for process selection. Process optimization considering all the responses has been carried out using gray relation grade analysis. This study aims at bridging the research gap in the application of AM machines for made to order situation prevalent in current industrial practice.

## 3.2 Experimental Details

### 3.2.1 CAD Model and STL File

The different internal structure geometries are shown in Fig. 3.2. CAD models of the

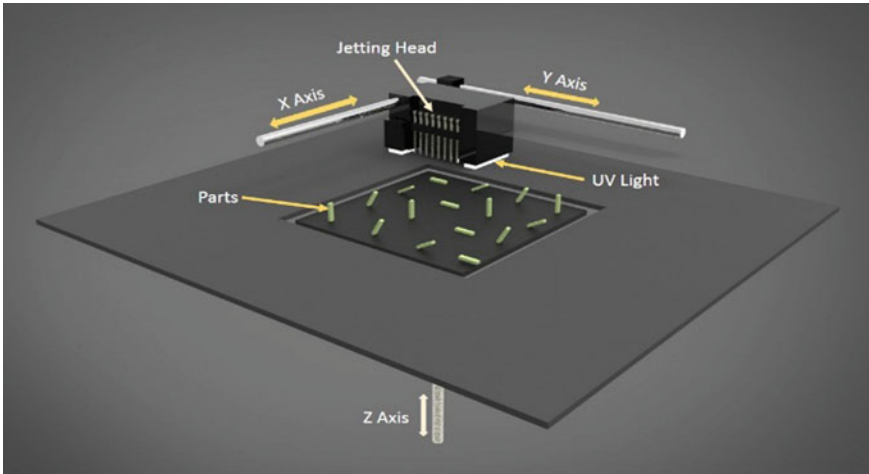


Fig. 3.1 Schematic representation of the PolyJet system

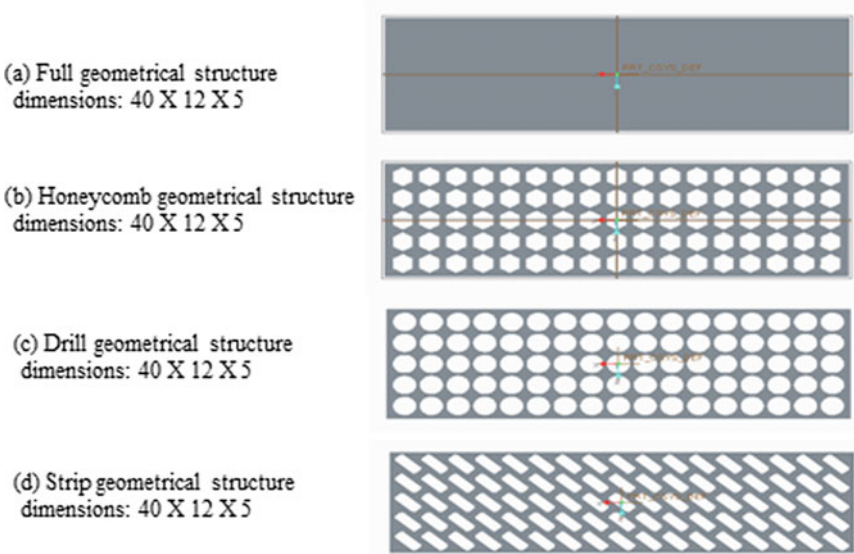


Fig. 3.2 Different internal structures, a full, b honeycomb, c drill, d strip

specimen are created using Creo Parametric 1.0, a popular CAD software (parametric technology corporation, USA). The CAD file is then exported as a standard tessellation language (STL) file. The standard parametric setting in the software (Creo) is used for STL file which are a coordinate system (default), format (ASCII with allowing negative values), and deviation control (chord height 0.1244 and angle control 0.5000).

### **3.2.2 Material**

Objet ABS-like digital material (RGD5160-DM) [10] which is composed of Objet RGD515 and Objet RGD535 are used in this work as test material. This material is widely used in the industries as a model material due to its inherent mechanical and thermal properties. Digital ABS is produced inside the PolyJet machine by mixing two liquid resins in equal proportions or as required depending on the properties desired. The support material is required for supporting the model while making and stabilizing subsequent model sections. This material is removed after the completion of a product by pressurizing the water jet. Gel-like photopolymer FullCure 705 has been used in this work as a support material.

### **3.2.3 Designs Build Tray Layout**

In PolyJet, AM machine parts are produced by depositing material layer upon layer on the built tray. The build tray area has been optimally designed to hold as many 16 specimens with orientations, different internal structure geometries, support structure, and surface finish. The tray is designed in such a way that the specimen length is oriented along the  $X$ -axis, the width along the  $Y$ -axis, and thickness parallel to the  $Z$ -axis. The tray design is shown in Fig. 3.3.

### **3.2.4 Preparation of Test Specimen**

For this work, test specimen having different internal structures (full, honeycomb, drill, and strip) have been designed. The nominal thickness of 5 mm, width 12 mm, and length 40 mm have been used to 3D printed specimens by the PolyJet system according to ASTM specifications for dynamic mechanical properties evaluation as shown in Fig. 3.4. Four internal structures (full, honeycomb, drill, and strip) for test specimens have been used here for experimental investigation.

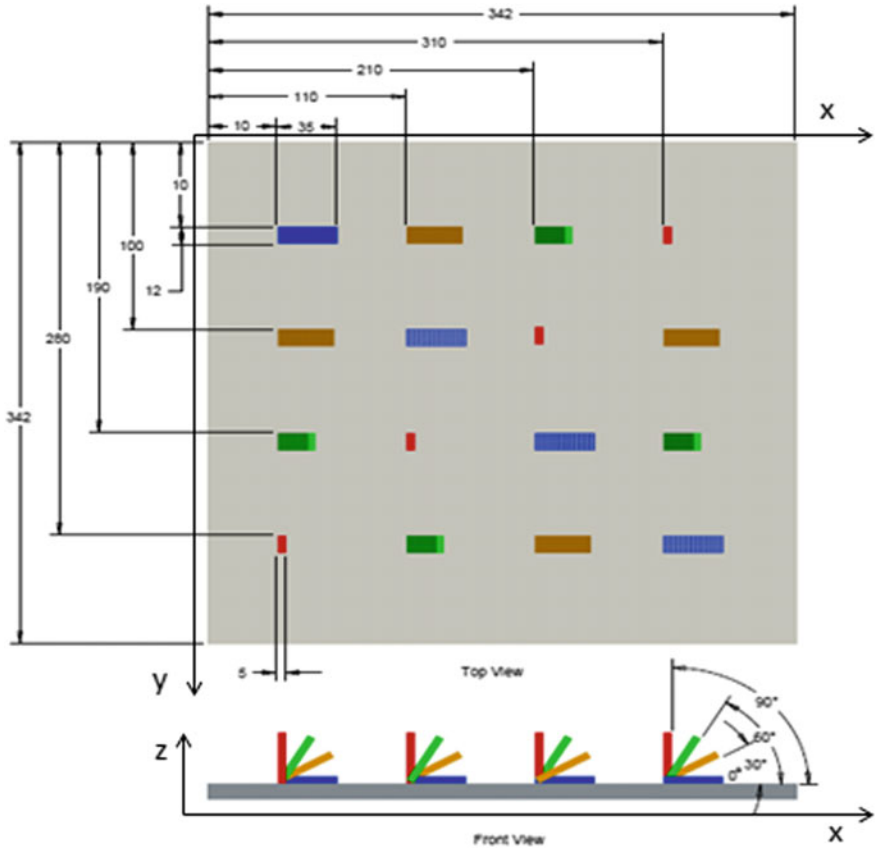


Fig. 3.3 Designs build tray layout

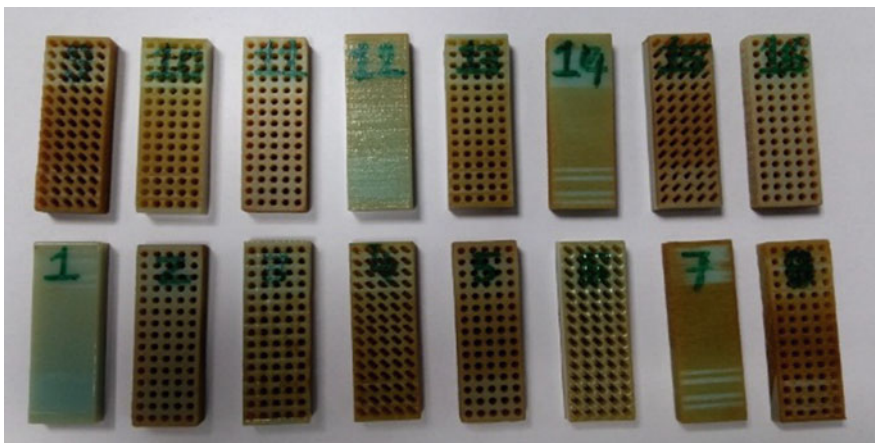


Fig. 3.4 3D printed specimens by the PolyJet system

### 3.2.5 Experimental Planning: Factors and Levels

Present work explores experimental investigation of PolyJet AM process using Connex 350 machine. Experiments have been carried out using L16 orthogonal mix array, comprising of 2-level arrays and 4-level arrays. The Taguchi method is useful in limiting the number of experiments and the optimal parameter setting. Six control factors have been varied in the present work in order to study their influence on response parameters. Control parameters and their levels are shown in Table 3.1 and explained in subsequent paragraphs. Experimental design and response parameters are shown in Table 3.2.

**Part spacing along the X-axis ( $\Delta x$ ):** In PolyJet, AM process parts are produced by adding very thin layers over layers on the build tray and are a very time-consuming process. In order to utilize the machine effectively, it is recommended to produce multiple parts in a single build tray. The machine has the capability to produce multiple parts simultaneously and thus can be used efficiently, reducing the time consumption per parts considerably. Therefore, part placement on building tray is important to optimally utilize the build tray area to produce the maximum number of parts in a single build tray. The net built tray volume used for this work is  $342 \times 342 \times 200$  mm. To select the proper part spacing, it is necessary to consider the size and dimension of parts, its orientation, and avoidance of superposing of the support material of two adjacent parts. Four levels of part spacing are considered for this experiment viz. 10, 110, 210, and 310 mm. With this spacing, four parts shall be manufactured along the X direction.

**Part spacing along the Y-axis ( $\Delta y$ ):** Part spacing along the Y-axis shares the same minimum limit with X spacing. However, the maximum limit could have reached an 80 mm value, since the test part width allowed for a higher spacing than the

**Table 3.1** Control parameters and their levels

Symbols	Control parameters	Unit	Levels			
			1	2	3	4
$\Delta x$	Part spacing along the X-axis	mm	10	100	190	280
$\Delta y$	Part spacing along the Y-axis	mm	10	110	210	310
$\theta$	Orientation of the part within the tray	Degree	0	30	60	90
ISG	Internal structure geometry		Full	Honeycomb	Drill	Strips
SS	Support structure		Heavy	Lite		
SF	Surface finish		Glossy	Matte		

*F* full; *H* honeycomb; *S* strip; *D* drill; *H* heavy; *L* lite; *G* glossy; *M* matte

$\Delta x$  part spacing along X-axis;  $\Delta y$  part spacing along Y-axis;  $\theta^\circ$  part orientation; *ISG* internal structure geometry; *SS* support structure; and *SF* surface finish

**Table 3.2** Taguchi mixed level design L16 orthogonal array and measured output responses

Run	Factors					Responses					
	$\Delta x$	$\Delta y$	$\theta$	ISG	SS	SF	Storage modulus MPa	Loss modulus MPa	Loss factor Tan $\delta$	Glass transition temp. (T <sub>g</sub> ) °C	Surface roughness (Ra)
1	10	10	0°	F	H	G	634	14	0.0222	112.8	0.279
2	10	110	30°	H	H	M	272	18	0.0667	73.7	10.880
3	10	210	60°	D	L	G	345	17	0.0495	90.8	1.540
4	10	310	90°	S	L	M	188	9	0.0492	86	6.861
5	100	10	30°	D	L	M	254	16	0.0641	74.3	11.667
6	100	110	0°	S	L	G	404	12	0.03	98.5	0.392
7	100	210	90°	F	H	M	516	22	0.0423	93.8	13.700
8	100	310	60°	H	H	G	263	15	0.0583	78.2	3.255
9	190	10	60°	S	H	M	170	11	0.065	75.6	13.645
10	190	110	90°	D	H	G	279	14	0.0504	84.4	0.828
11	190	210	0°	H	L	M	312	17	0.0535	78.9	9.195
12	190	310	30°	F	L	G	610	20	0.0334	98.7	2.171
13	280	10	90°	H	L	G	317	14	0.0432	91.9	1.091
14	280	110	60°	F	L	M	528	24	0.046	97.1	14.098
15	280	210	30°	S	H	G	232	10	0.0446	85.8	1.023
16	280	310	0°	D	H	M	343	15	0.0451	86.8	5.669

previous factor. Nevertheless, the same limits and levels (10, 100, 190, and 280 mm) previously defined in the  $X$  direction spacing had been used for convenience.

The orientation of the part within the tray ( $\theta$ ): Due to symmetries involved, the orientation of the part within the tray can be limited for testing purposes between  $0^\circ$  and  $90^\circ$ . Test specimen already has  $180^\circ$  symmetry and, due to manufacturing strategy, possible differences in UV curing between zones of the same part are expected to be distributed in a specular pattern, in parts oriented symmetrically with respect to the  $YZ$  plane. According to this consideration, the test specimen rotated  $90^\circ$  is expected to present identical mechanical behavior. Internal structure geometry (ISG): Four types of internal structure geometry (full, honeycomb, drill and strip) are used for this experiment. According to this consideration, test specimens are expected to present different mechanical behavior. The support structure (SS): Three types of a grid are used as the support structure in PolyJet processed parts. The PolyJet technology offers three options for support structure: Standard, heavy, and lite can be related to the strength of the part.

Surface finishes (SF): Finally, the surface finish of PolyJet parts can be related to roughness profile but, in the particular case of flat surfaces parallel to the  $XY$  plane, differences in roughness shall be almost negligible. Nevertheless, the PolyJet technology offers two options for the surface finish: glossy and matte. Unsupported surfaces can be manufactured using either option since matte finishing can be obtained by applying a thin coating of support material over a glossy surface. On the other hand, supported surfaces are always matte, since contact between support and construction materials cannot be avoided. It is not clear how this additional coating should affect the mechanical properties of matte surfaces when compared to glossy ones.

### 3.3 Results and Discussion

#### 3.3.1 Analysis of Storage Modulus

Storage modulus is the elastic property of polymer material. The main effects plot for the SN ratios of storage modulus is shown in Fig. 3.5. The storage modulus is mainly affected by part orientation and internal structure geometry. Storage modulus is found to be decreasing as part orientation varies from  $0^\circ$  to  $90^\circ$ . Storage modulus exhibits maximum value at  $0^\circ$  because of the orientation of part length along the  $X$ -axis. Storage modulus found to be on the higher side when the internal structural geometry is set at full structure, whereas storage modulus is least when the internal structural geometry is set at strips structure. ANOVA for storage modulus is carried out and the values obtained of  $R$ -sq = 98.36% and  $R$ -sq(adj) = 75.35%.



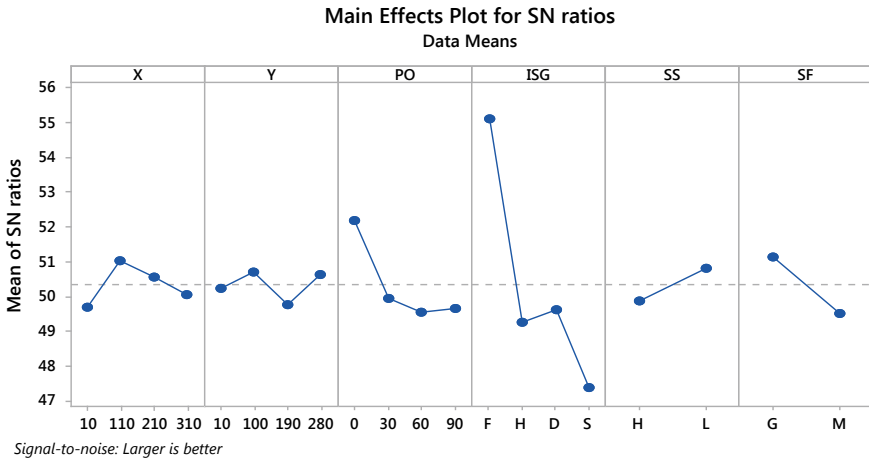


Fig. 3.5 S/N ratio plot for storage modulus

### 3.3.2 Analysis of Loss Modulus

Loss modulus defines the viscous property of the material. The main effects plot for the SN ratios of the loss modulus is shown in Fig. 3.6. Loss modulus found to be mainly affected by internal structure geometry. It is observed that loss modulus is minimum when the internal structural geometry is set at strips structure. Other variables are found to be the least significance. ANOVA for loss modulus is carried out and the values obtained of  $R\text{-sq} = 97.83\%$  and  $R\text{-sq(adj)} = 67.52\%$ .

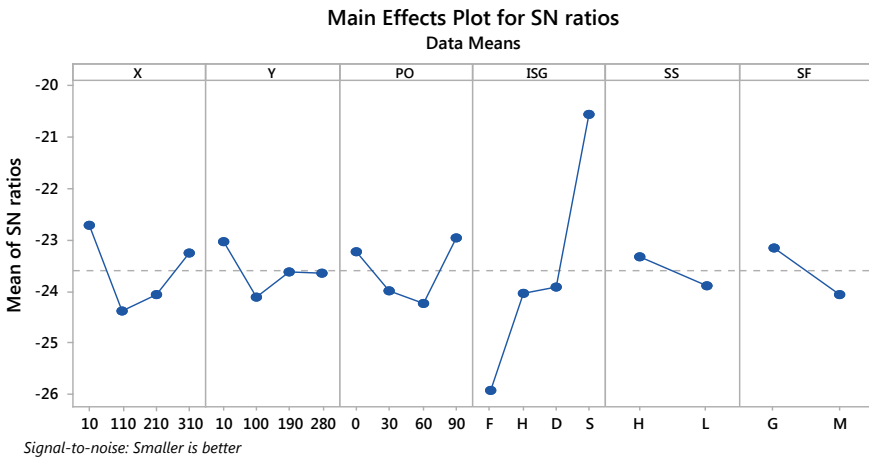


Fig. 3.6 S/N ratio plot for loss modulus

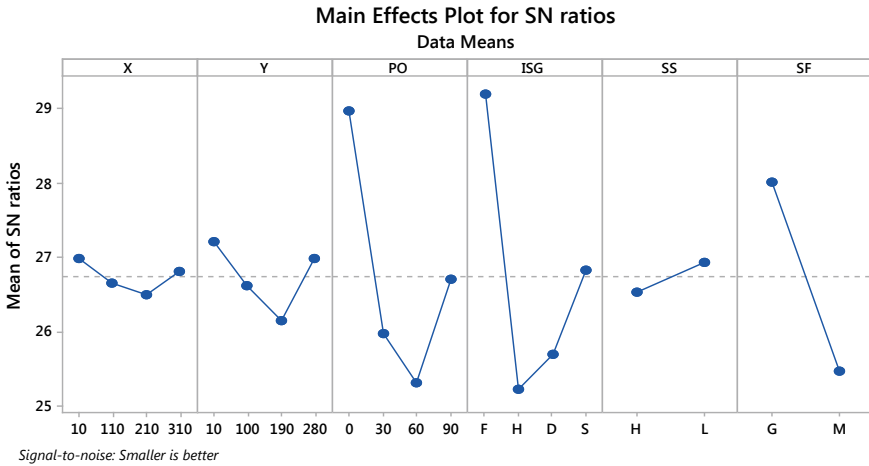


Fig. 3.7 S/N ratio plot for loss factor

### 3.3.3 Analysis of Loss Factor

Main effects plot for the SN ratios of loss factor is shown in Fig. 3.7. The loss factor is the ratio of the loss modulus to the storage modulus. The loss factor is found to be affected by partial orientation, internal structure geometry, and surface finish. Due to the orientation of part length along the X-axis, loss factor is minimum when part orientation set at 0°, internal structure geometry set at full structure, and surface finish is set on glossy. ANOVA for loss factor is carried out and the values obtained of  $R\text{-sq} = 99.54\%$  and  $R\text{-sq(adj)} = 93.08\%$ .

### 3.3.4 Analysis of Glass Transition Temperature

Figure 3.8 shows the main effects plot for the SN ratio of glass transition temperature. The glass transition temperature is one of the most important properties of polymers and is the temperature region where the polymer transitions from a hard, glassy material to a soft, rubbery material. Glass transition temperature is found to be affected by part spacing along the Y-axis, part orientation, internal structure geometry, and surface finish. Part spacing along the Y-axis is an important factor in this study, due to layer deposition method of PolyJet technology. In PolyJet technology, the layer is deposited by nozzles in the raster scan method. Nozzles start depositing layer from origin and moves in X-direction. After completing one travel along the X-axis, it returns to start of deposition and increments in Y direction and deposits material in the same manner till full build tray is covered. It would require more deposition cycles per layer as a result for each layer available curing time is more.

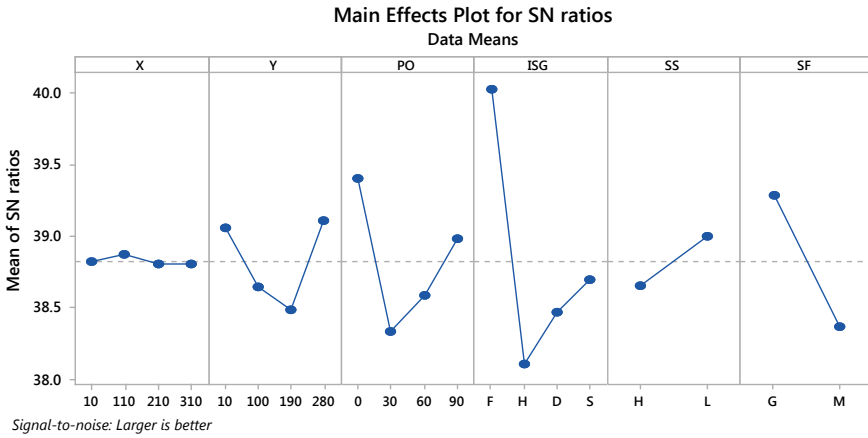


Fig. 3.8 S/N ratio plot for glass transition temperature

ANOVA for glass transition temperature is carried out and the values obtained of  $R\text{-sq} = 99.45\%$  and  $R\text{-sq(adj)} = 91.79\%$ .

### 3.3.5 Analysis of Surface Roughness

Main effects plot for the SN ratios of surface roughness is shown in Fig. 3.9. Surface roughness is mainly affected by part orientation and surface finish. Surface roughness value of the prepared samples found to be less when a part is orientated at  $0^\circ$  With

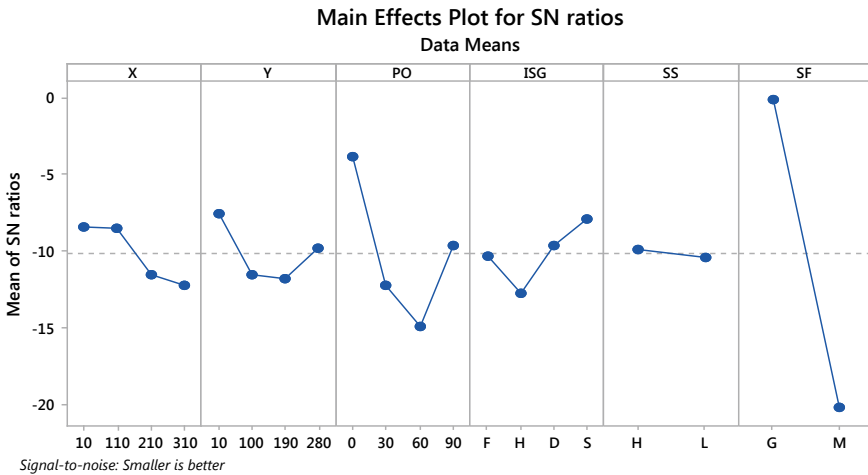


Fig. 3.9 S/N ratio plot for surface roughness

respect to  $Y$ -axis and surface finish is glossy. It is found that support material is deposited only in contact with bed lower surface of the sample, while parameters such as glossy mode are selected and the part length is oriented along the  $X$ -axis. ANOVA for surface roughness is carried out and the values obtained of  $R$ -sq = 99.95% and  $R$ -sq(adj) = 99.23%.

### 3.4 Optimization of Parameters Using GRG

Gray relation grade analysis is used to optimize the process parameters for the PolyJet process. GRG analysis is the most effective tool for multi-attribute decision-making, which converts the multiple responses into a single grade. The following steps are followed to calculate the GRG and multi-attribute decision-making:

- Step 1 Calculation of S/N ratio for giving observations. In the PolyJet process, the objective is to reduce the loss modulus, loss factor, and surface roughness. Hence, smaller the better criteria have been applied to loss modulus, loss factor, and surface roughness. To increase the storage modulus and glass transition temperature larger the better criteria have been applied.
- Step 2 Normalization of data.
- Step 3 Computation of Grey Relation co-efficient
- Step 4 Computation of Grey Relational Grade.
- Step 5 Taguchi analysis of GRG to get the optimal parameter setting.
- Step 6 Confirmatory experiments to validate the optimal settings of input parameters

The computed values of GRG are given in Table 3.3 and the main effects plot for SN ratios of GRG is shown in the Fig. 3.10. From the main effects plot it is observed that the optimal parameter setting in part spacing along the  $X$  axis at 0 mm, part spacing along the  $Y$  axis at 37.32 mm, the orientation of the part within the tray at  $0^\circ$ , internal structure geometry is full, the support structure is a lite, and matte surface finish is the optimal GRG. ANOVA for GRG is carried out and the values obtained of  $R$ -sq = 99.93% and  $R$ -sq(adj) = 98.91%. These optimal conditions are further validated by confirmatory experiments and found to be well within permitted variation.

**Table 3.3** Grey relational grade (GRG)

Exp. No.	1	2	3	4	5	6	7	8	9	10	11	12	13	14	15	16
GRG	0.99	0.92	0.95	0.94	0.92	0.97	0.94	0.94	0.92	0.95	0.93	0.97	0.96	0.93	0.95	0.95

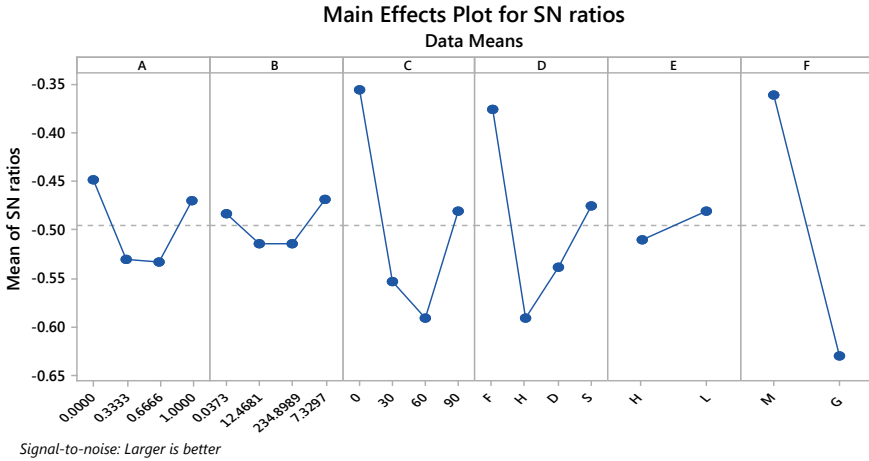


Fig. 3.10 Main effects plot for SN ratios of GRG

### 3.5 Conclusions

This research presented the analysis of the variability of mechanical properties in PolyJet-manufactured rectangular bars, regarding its pre-defined distribution pattern on the manufacturing tray. Rectangular bars have been used for testing purposes and later manufactured with a Stratasys Objet 350 machine. Subsequently, storage modulus, loss modulus, loss factor, Glass Transition Temperature, and surface roughness have been measured. Analyzed the following conclusions are drawn from this work:

- Storage modulus mainly affected by part orientation and internal structure geometry. Storage modulus is found to be decreasing as part orientation varies from 0° to 90°. Storage modulus exhibits maximum value at 0° because of the orientation of part length along the X-axis. Also, the storage modulus found to be on the higher side when the internal structural geometry is set at the full structure, whereas the storage modulus is least when the internal structural geometry is set at strips structure.
- Loss modulus found to be mainly affected by the internal structure geometry. It is observed that loss modulus is minimum when the internal structural geometry is set at Strips structure. Other variables are found to be the least significance.
- The loss factor is found to be affected by part orientation; internal structure geometry and surface finish. Due to the orientation of part length along the X-axis. The loss factor is minimum when the part orientation set at 0°, internal structure geometry set at full structure and surface finish is set on glossy.
- Glass transition temperature is found to be affected by part spacing along the Y axis, part orientation, internal structure geometry, and surface finish. Part spacing along the Y-axis, it would require more deposition cycles per layer as a result for

each layer available curing time is more. It is found that orientation of the part length along the  $X$  axis results in an increase in glass transition temperature.

- Surface roughnesses are mainly affected by part orientation and surface finish. Surface roughness value of the prepared samples found to be less when part orientated  $0^\circ$  and surface finish is glossy. This is found that the orientation of part length along the  $X$ -axis and selection of glossy mode deposits support material only in contact with the bed and lower surface of the sample.

From the GRG analysis, it is observed that optimal parameters setting for PolyJet 3D printing of ABS material are part spacing along the  $X$  axis at 0 mm, part spacing along the  $Y$  axis at 37.32 mm, the orientation of the part within the tray at  $0^\circ$ , internal structure geometry is full, the support structure is a lite, and matte surface finish.

## References

1. Wohlers, T.: Wohlers Report—Annual Worldwide Progress Report—Additive Manufacturing and 3D Printing State of the Industry. Wohlers Associates (2014)
2. Santos, E.C., Shiomi, M., Osakadaa, K., Laoui, T.: Rapid manufacturing of metal components by laser forming. *Int. J. Mach. Tools Manuf.* **46**, 1459–1468 (2006)
3. Mellor, S., Hao, L., Zhang, D.: Additive manufacturing: a framework for implementation. *Int. J. Prod. Econ.* **149**, 194–201 (2014)
4. Clemon, L., Sudradjat, A., Jaquez, M., Krishna, A., Rammah, M., Dornfeld, D.: Precision and energy usage for additive manufacturing, volume 2A: advanced manufacturing. USA: ASME International Mechanical Engineering Congress and Exposition, San Diego, California(2013)
5. Gibson, I., Rosen, D. W., Stucker, B.: Additive manufacturing technologies—rapid prototyping to direct digital manufacturing. Springer (2010)
6. Dimitrov, D., van Wijck, W., Schreve, K., de Beer, N.: Investigating the achievable accuracy of three-dimensional printing. *Rapid Prototyp. J.* **12**(1), 42–52 (2006)
7. Brajlilh, T., Valentan, B., Balic, J., Drstvensek, I.: Speed and accuracy evaluation of additive manufacturing machines. *Rapid Prototyp. J.* **17**(1), 64–75 (2010)
8. Anand, S., Ratnadeep, P.: Optimal part orientation in Rapid Manufacturing process for achieving geometric tolerances. *J. Manuf. Syst.* **30**, 214–222 (2011)
9. Pham, D., Gault, R.: A comparison of rapid prototyping technologies. *Int. J. Mach. Tools Manuf.* **38**, 1257–1287 (1998)
10. <http://www.stratasys.com/materials/material-safety-data-sheets/polyjet/digital-abs-materials>